www.rericjournal.ait.ac.th

Design of Low Voltage Ride through Control Method for Power System with New Energy Photovoltaic Access

Hua Ye*, ^, 1, Xinchen Lu^, Li Lin^, Wenbo Shi^, and Xinmiao Gong^

ARTICLE INFO

Article history:
Received 16 July 2025
Received in revised form
18 September 2025
Accepted 25 September 2025

Keywords:
Grid connected operation
Low voltage ride through
Model predictive control
New energy photovoltaic access
Power limiting control

ABSTRACT

In order to address the issue of DC bus voltage instability caused by the slow dynamic response of low-voltage ride-through (LVRT) control in power systems integrated with renewable photovoltaic (PV) energy, this paper proposes an active power-based direct control strategy for enhanced LVRT performance. The strategy begins by analyzing the LVRT requirements for such systems and examines the typical two-stage grid-connected PV system topology. Depending on the severity of the grid voltage sag, it calculates the reference power for both AC and DC sides, and then directly and actively controls the PV array and inverter to output the corresponding reference power, thereby rapidly balancing power on both sides. Experimental results show that under the proposed control method, when the grid voltage drops to 0.85 per unit (pu), the output power of the PV array is maintained at approximately 0.625 pu, demonstrating that the PV system can remain connected to the grid during voltage dips while providing reactive power compensation to help restore the grid voltage. This achieves effective LVRT control with improved dynamic performance.

1. INTRODUCTION

With the increasing installed capacity of photovoltaic (PV) power stations in China, the integration of PV energy into the grid is becoming increasingly common. Once a fault occurs in the distribution line, it will cause instantaneous peak current in the power grid, which will have a huge impact on converters and other devices [1]-[2]. Adopting passive protection measures may lead to a significant decrease in the active output of photovoltaic power plants, and in severe cases, even the spread of power grid faults, resulting in the disconnection of other power plants and causing large-scale power outages [3]. Therefore, following the introduction of new grid codes for photovoltaic power plants in China, it is required that they possess robust low-voltage ride-through (LVRT) capabilities to ensure the continuity of grid-connected operation during grid faults.

Sun *et al.* [4] first established a full order large signal model of photovoltaic inverters to solve the thorny problem of transient instability during severe voltage drops in weak power grids. Then, based on the established model, analysis shows that in weak power grids, inverters will face the risk of losing stability due to current transients during low voltage ride through periods. By studying the influence of a low short-circuit ratio (SCR) on the attraction region of the post-fault equilibrium point, the inherent mechanism of inverter instability under weak grid conditions was revealed. However, the stability performance of the method itself requires improvement. Zheng *et al.* [5] proposes a machine grid coordinated control strategy based on model predictive current control to address the problem of traditional new energy photovoltaic connected power storage systems during grid faults. This technology has excellent dynamic characteristics, which can enable the output current of the grid side inverter to quickly follow the reference current command. During voltage dips in the power grid, when the grid side inverter uses a model predictive current control current inner loop instead of a proportional integral current inner loop, the low voltage ride through capability of the energy storage system will be improved. However, the effectiveness of this method in controlling the sustainability of low voltage ride through needs to be improved. Ni *et al.* [6] proposes a novel low switching frequency control strategy for the active front-end of a regenerative cascaded H-bridge driver with low voltage ride through capability. By utilizing the existing phase-shifting transformer in the drive, the main harmonic components generated by the active front-end under the proposed control strategy can be eliminated, demonstrating good performance in power system LVRT control applications. Pal *et al.* [7] proposes a new current saturation strategy based on grid forming inverters. The proposed control concept limits the output current during low voltage ride through periods through a new control parameter - power factor angle, thereby enabling the inverter to comply with one of the standardized grid specifications. Firstly, a nonlinear mathematical model was established that captures the full order average dynamics of the inverter

DOI: https://doi.org/10.64289/iej.25.0412.4858769

*Tianjin University, Tianjin 300072, China.

^Yunnan Power Grid Co., Ltd, Kunming, Yunnan 650200, China.

[1]Corresponding author;
E-mail: yehualunwen@163.com

with embedded current limiting control. Subsequently, a simplified equivalent circuit model was established, but the control effect of this method on the stability of inverter low-voltage ride through state control was poor.

Based on this, this paper innovatively proposes a low voltage ride through strategy, which aims to solve the problems of slow dynamic response and DC bus voltage instability existing in the traditional strategy when dealing with the power system with new energy photovoltaic access. Through in-depth analysis of power system LVRT requirements and the topology of grid-connected PV systems, this strategy calculates reference power for both the AC and DC sides based on the voltage sag depth. It then directly controls the PV array and inverter to output the corresponding reference power, thereby rapidly achieving power balance between the AC and DC sides. This strategy not only improves the low voltage ride through capability of photovoltaic power plants, but also ensures the continuity and stability of grid connected operation of photovoltaic power plants during grid failure, and provides new ideas and methods for grid connected utilization of new energy. The research results of this paper are of great significance to promote the development of new energy photovoltaic industry and improve the operation efficiency and reliability of power system.

2. DESIGN OF LOW VOLTAGE RIDE THROUGH CONTROL METHOD FOR POWER SYSTEM

2.1 Low Voltage Ride through Requirements of Power System with New Energy Photovoltaic Access

The power system connected to new energy photovoltaic access refers to the overall system that connects photovoltaic into the power network in different ways, mainly including off grid access and grid connected access [8]-[9]. The system mainly consists of photovoltaic power sources (photovoltaic cell arrays), power conversion equipment (such as DC-DC converters, DC-AC inverters, *etc.*), control equipment, energy storage equipment (some systems include), transmission lines, and loads. After many large photovoltaic power plants, they not only meet the regional electricity demand, but also achieve remote transmission of electricity through ultra-high voltage transmission lines.

In the current utilization of new energy photovoltaic access, a large number of photovoltaic power stations are connected to the power system through grid connection. Whether it is large centralized photovoltaic power stations or numerous distributed photovoltaic power stations, they are generally connected to the grid in a grid connected manner. From this, it can be seen that the photovoltaic grid connected power system formed, occupying a large scale in the new energy photovoltaic grid connected power system.

Low voltage ride through (LVRT) refers to the ability of an inverter to operate continuously without disconnecting from the grid within a certain range when the AC output voltage of the inverter drops due to system faults or disturbances. It is an important indicator for measuring the stable operation capability [10]-[11]. Low voltage ride through capability refers to the ability of the grid voltage drops due to various faults such as short circuits, in order to ensure the grid connected operation. When the voltage drops to a certain extent, the photovoltaic power plant is required to inject a certain [12]. The State Grid Corporation of China has formulated specific grid code requirements for photovoltaic power stations during LVRT events, clearly defining the operational standards. The specific content of the standards is shown in Figure 1.

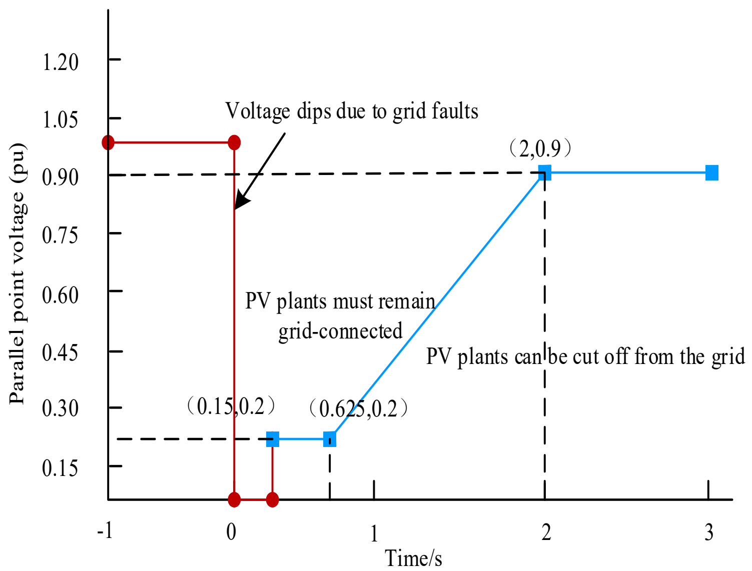

Fig. 1. Operation specifications of photovoltaic power station during low voltage ride through period.

As shown in Figure 1, during the voltage ride through period, the operating standards of the photovoltaic power station indicate that when the grid voltage drops, if the grid voltage is above the contour line, the photovoltaic power station must maintain grid connected operation; When the voltage at the grid connection point drops to 0 seconds, the photovoltaic system is required to be able to continue grid connected operation within 0.15 seconds; When the voltage at the grid connection point drops to 20% of the rated voltage, the photovoltaic system is required to be able to continue grid connected operation for 0.625 seconds, and the photovoltaic power generation system is required to recover to 90% of the rated voltage within 2 seconds of the voltage drop; If the voltage at the grid connection point drops below the voltage contour line, the photovoltaic power station can be disconnected from the grid.

2.2 Topology Analysis of Power System for New Energy Photovoltaic Access

According to the low - voltage ride - through requirements of the new energy photovoltaic access power system depicted in Figure 1, when considering the overall structure of the photovoltaic grid - connected power system, an analysis of the traditional two - level photovoltaic grid - connected power system topology (as shown in Figure 2) is carried out as follows:

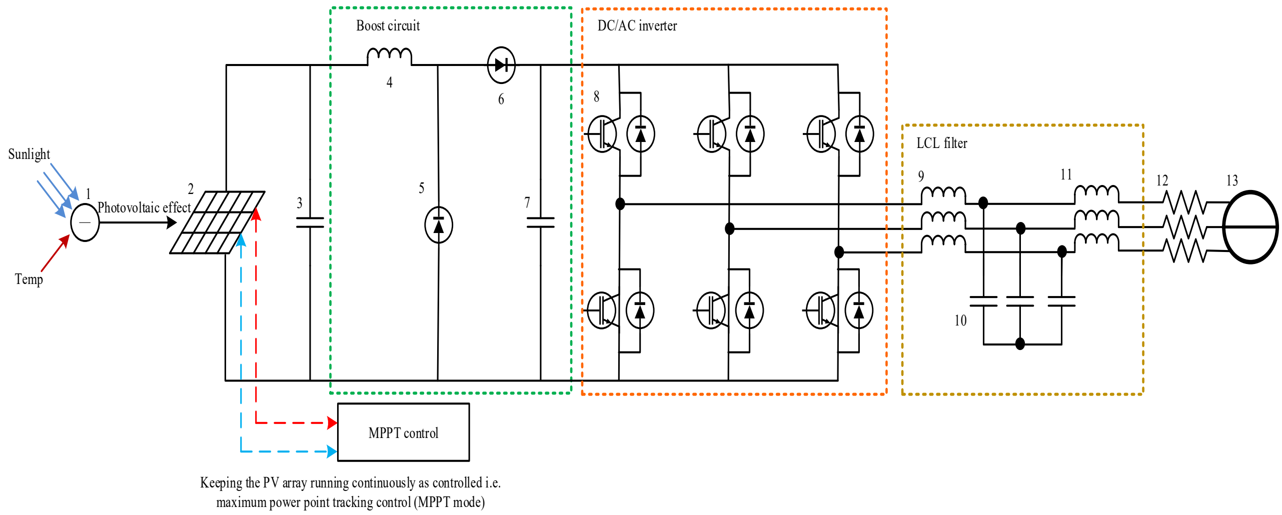

Fig. 2. Topology structure of traditional two-stage photovoltaic grid connected power system.

As shown in Figure 2, the traditional two-stage photovoltaic grid connected power system topology mainly presents the layout structure and electrical function relationship of elements such as 1 Photon unit, 2 Solar cell photovoltaic array, 3 PV array input side capacity, 4 Energy storage conductors, 5 Converter bridge arm (bridge circuit branch), 6 Diode, 7 DC bus capacity for photovoltaic power plants, 8 Inverter bridge arms, 9 Inverter side induction, 10 AC side filter capacitor, 11 Network side induction, 12 Filter resistors, 13 Grid, *etc*.

Its topology mainly includes the front-end circuit of the photovoltaic power generation system composed of photovoltaic arrays and Boost circuits, as well as the back-end circuit structure composed of three-phase AC power grid, *etc*. [13]-[15]. In the front - end circuit structure, the maximum power point tracking (MPPT) of the photovoltaic array is realized by controlling the duty cycle of the Boost circuit switch. In the rear - end circuit structure, the stability of the DC - side voltage of the inverter depends on the voltage outer loop, and the current inner loop is utilized to make the grid current track the grid voltage with the same frequency and phase, namely, unity power factor grid - connection [16]. Under normal grid voltage conditions, the grid voltage and grid-connected current are measured. The AC quantities in the three-phase stationary coordinate system (abc) are then transformed into DC quantities in the two-phase rotating reference frame (dq) through coordinate transformation (*e.g.*, Park-Clarke transformations).

2.3 Low Voltage Ride through Control Method for Power System with New Energy Photovoltaic Access

2.3.1 Traditional low-voltage ride through strategy

According to the topology structure shown in Figure 2, it can be observed that for the above - mentioned two - stage photovoltaic grid - connected power system, the Boost circuit is capable of isolating the photovoltaic power station from the grid - connected inverter. When the grid voltage drops, if the photovoltaic array keeps operating in MPPT mode, it means that the output power decreases due to the drop in grid voltage. In order to maintain power balance, excess energy will accumulate in the DC side capacitor of the inverter, causing voltage rise and even overvoltage [17]-[18]. Meanwhile, due to the imbalance of power on both sides of the inverter, it can cause an increase in grid side current, even exceeding the tolerance range of power electronic devices, leading to the generation of overcurrent [19]. Therefore, in order to ensure the grid connected operation of photovoltaic power generation systems during voltage drops, it is necessary to limit the DC side voltage and grid side current.

Firstly, based on the structure of Figure 2, the two-stage photovoltaic grid connected mathematical model under the d and q rotation coordinate axes is defined as:

$$\vec{U}_d = \delta_1 \vec{I}_d - \delta_2 \delta_1 \vec{I}_q + \vec{U}'_d + \delta_3 \frac{\mathrm{d}\vec{I}_d}{\mathrm{dt}} \quad (1)$$

$$\vec{U}_q = \delta_1 \vec{I}_q - \delta_2 \delta_1 \vec{I}_d + \vec{U}'_q + \delta_3 \frac{\mathrm{d}\vec{I}_q}{\mathrm{dt}} \quad (2)$$

In the formula: $\vec{U}_d$、$\vec{U}_q$ represents the d and q-axis components of the grid side voltage, and represents the projection of the grid voltage on the d-axis and q-axis; $\vec{I}_d$、$\vec{I}_q$ represents the d-axis and q-axis components of the grid side current, and represents the projection of the current injected by the inverter into the grid on the d-axis and q-axis; δ_1、δ_2、δ_3 represents the angular frequency of the filtering inductor, filtering resistor, and photovoltaic grid connected power system, which together determine the dynamic characteristics of the system; $\vec{U}'_d$、$\vec{U}'_q$ represents the d-axis and q-axis components of the inverter side voltage, indicating the voltage generated by the inverter on the d-axis and q-axis..

Based on the two-stage photovoltaic grid connected mathematical model that integrates formulas (1) and (2). In accordance with the instantaneous power theory, the analysis of the active and reactive power injected into the grid by the inverter is carried out as follows:

$$\vec{P}'_0 = 1.5\left(\vec{U}_d \vec{I}_d + \vec{U}_q \vec{I}_q\right) \quad (3)$$

$$\vec{Q}'_0 = -1.5\left(\vec{U}_d \vec{I}_d - \vec{U}_q \vec{I}_q\right) \quad (4)$$

In the formula: $\vec{P}'_0$ represents the active power injected by the inverter into the photovoltaic grid, and represents the useful power transmitted by the inverter to the grid; $\vec{Q}'_0$ represents the reactive power injected by the inverter into the photovoltaic grid, and represents the reactive power exchanged between the inverter and the grid.

Based on the analysis results in Figure 1, the active power delivered by the inverter to the grid side will decrease [20]. At this point, if the front-end circuit is still operating in MPPT mode, there will be a power difference between the DC and AC sides, and power redundancy will accumulate on the DC bus, causing the DC bus voltage to be too high and triggering overvoltage protection, resulting in photovoltaic disconnection [21]. At this point, if the losses of the inverter and AC side filter are not considered, the balance formula for the DC bus voltage can be expressed as:

$$\vec{P}_1 = \vec{P}'_0 + 0.5\hat{c}_0 \times \frac{\mathrm{d}\left(\hat{U}_0\right)^2}{\mathrm{dt}} \quad (5)$$

In the formula: $\vec{P}_1$ represents the output power of the photovoltaic side, and represents the power generated by the photovoltaic array; $\hat{c}_0$ represents the DC bus capacitor, which is used to smooth out fluctuations in the DC bus voltage; $\hat{U}_0$ represents the DC bus voltage and the voltage level on the DC bus.

Based on the two-stage photovoltaic grid connected mathematical model presented in formulas (1) - (5), conduct a correlation analysis of traditional low-voltage ride through strategies. In the traditional low-voltage ride through (LVRT) control process on the DC side, when LVRT occurs, the grid voltage drops, and due to current limiting, the power delivered by the inverter to the grid decreases [22]. If the previous stage is still operating under MPPT control, it will cause the DC bus voltage to pump up, triggering overvoltage protection, and the DC side Boost circuit will switch from MPPT control to constant voltage control [23]. This is mainly due to the passive adjustment of DC bus voltage fluctuations, resulting in slow dynamic response speed. However, under this control strategy, the decrease in photovoltaic output power is due to the passive adjustment of DC bus voltage fluctuations, resulting in slow dynamic response speed.

On the AC side, traditional LVRT control switches from unity power factor mode to reactive power compensation mode. At this point, a proportional integral controller (PI) is deployed in the AC side control architecture to precisely adjust the dq component of the grid connected current. By conducting proportional and integral operations on the current error (the difference between the actual current and the reference current), an appropriate control signal is generated to adjust the output of the inverter, enabling the grid - connected current to track the reference current. First of all, the grid - connected current component is expressed as:

$$\vec{I}'_d = \frac{\vec{P}_1}{\vec{U}'_d}, \vec{I}'_d \geq 1.5\left(\vec{I}'_0 - 1\right) \quad (6)$$

$$\vec{I}'_q = -K_q\left(\vec{U}'_q - \overline{U}'_0\right), \overline{U}'_0 \leq 0.2 \quad (7)$$

In the formula, $\vec{I}'_d$、$\vec{I}'_q$ represents the d-axis and q-axis components of the inverter side current, indicating the current that the inverter should output in the d-axis and q-axis directions; $\vec{I}'_0$ represents the rated value of grid connected current, used for standardization, that is, converting the actual current into a proportion relative to the rated value; K_q represents the droop control coefficient in the q-axis direction, used to adjust the output of reactive power; $\overline{U}'_0$ represents the amplitude of the voltage at the grid connection point, used for standardization, that is, converting the voltage to a ratio relative to the rated voltage.

Secondly, in traditional communication side LVRT control, due to the need to consider closed-loop bandwidth issues, the inner loop speed cannot be set too fast, which can result in slower dynamic response speed when $\vec{P}_1$ and $\vec{I}_0'$、$\vec{U}_0'$ change.

2.3.2 DC side LVRT control strategy for photovoltaic grid connected power system

In order to ensure that the reference power can be quickly tracked to achieve balance between the AC and DC sides when a fault occurs, this paper proposes an adaptive real-time tracking method for the power reference value [24]. Firstly, calculate the power reference value based on the degree of voltage drop in the power grid:

$$\vec{P}'' = \vec{P}_1 \lambda_1 \times \frac{\widetilde{U}_1'}{\vec{U}_0''} \times \widetilde{I}_{max}'' \tag{8}$$

$$\lambda_1 = \sqrt{\left(\vec{P}_0' + \vec{Q}_0'\right)^2}^{\,-1} \times \vec{P}_1 \tag{9}$$

In the formula, $\vec{P}''$ represents the power reference value, which indicates the power that the inverter should output when the grid voltage drops; λ_1 represents the per unit value of the maximum output current of the inverter, and represents the ratio of the maximum current that the inverter can output relative to the rated current; $\widetilde{U}_1'$ represents the effective value of the phase voltage on the AC side, indicating the actual magnitude of the grid voltage; $\overleftarrow{U}_0''$ represents the rated phase voltage and the rated value of the grid voltage; λ_1 represents power factor, which is the ratio of active power to apparent power caused by the phase difference between the inverter output current and voltage.

Under normal operating conditions, the power factor can be further expressed by combining formulas (6) and (7) as follows:

$$\lambda_1 = \sqrt{\left(1.1\vec{I}_d' + \vec{I}_q'\right)^2}^{\,-1} \times \vec{I}_d', \vec{I}_q' = 0 \tag{10}$$

Under normal operating conditions, the d-axis component of the inverter side current is determined by the DC bus voltage control loop. At this time, the q-axis component of the inverter side current is set to 0, and the voltage reference value, voltage estimation value, and photovoltaic side output voltage are defined as u_1、u_2、u_3, respectively. Then, based on the power reference value, the corresponding power output of the photovoltaic is directly controlled. The control principle of the DC side LVRT is shown in Figure 3:

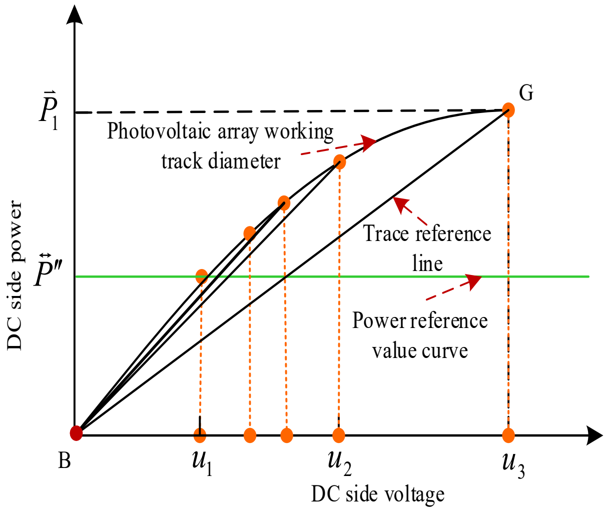

Fig. 3. Principle of fast tracking power reference value load shedding.

As shown in Figure 3, it is known that the operating point of the photovoltaic array is initially at point G, at which point the output power of the photovoltaic side is higher than the power reference value. Then, from the initial working point to the coordinate origin, draw a straight line as the maximum power point tracking reference line and a curve as the working path of the photovoltaic array [25]. Therefore, the voltage estimation value can be found by tracking the intersection point of the power reference value, and then the voltage estimation value can be set as the voltage reference value. By continuously repeating the above operation, the working point of the photovoltaic array moves along the working path of the photovoltaic array towards the voltage reference value. During this process, the output voltage of the photovoltaic side will not exceed the voltage reference value [26]. Therefore, the output voltage on the photovoltaic side will eventually converge to the voltage reference value, and the operating point be located at the intersection of the voltage reference value and the reference value, thereby achieving LVRT control on the DC side of the photovoltaic grid connected power system.

2.3.3 LVRT control strategy for AC side of photovoltaic grid connected power system

Based on the principle of model predictive control, a LVRT control strategy for the AC side of a photovoltaic grid connected power system is designed. The voltage formula for the AC side of the α - β three-phase system variable coordinate system is:

$$\delta_2 \frac{d\overleftarrow{I}_{\alpha\beta}''}{dt} = \vec{V}_{\alpha\beta}' - \left(\delta_1 \overleftarrow{I}_{\alpha\beta}'' + \overleftarrow{V}_{\alpha\beta}''\right) \tag{11}$$

In the formula: $\overleftarrow{I}_{\alpha\beta}''$ represents the α - β component of the grid connected current, which represents the current injected by the inverter into the grid in the alpha beta coordinate system; $\vec{V}_{\alpha\beta}'$ represents the alpha beta component of the inverter output voltage, which represents the voltage generated by the inverter in the alpha beta coordinate system; $\bar{V}''_{\alpha\beta}$ represents the alpha beta component of the grid voltage, which represents the voltage of the grid in the α - β coordinate system.

Perform forward Euler discretization on formula (11) to obtain a numerical solution for the multi-component grid connected current in discrete time:

$$\bar{I}''_{\alpha}(\hat{k}+1)=\bar{I}''_{\alpha}(\hat{k})+\delta_1^{-1}t'\left[\bar{V}'_{\alpha}(\hat{k})-\bar{V}''_{\alpha}(\hat{k})-\delta_2\bar{I}''_{\alpha}(\hat{k})\right] \quad (12)$$

$$\bar{I}''_{\beta}(\hat{k}+1)=\bar{I}''_{\beta}(\hat{k})+\delta_1^{-1}t'\left[\bar{V}'_{\beta}(\hat{k})-\bar{V}''_{\beta}(\hat{k})+\delta_2\bar{I}''_{\beta}(\hat{k})\right] \quad (13)$$

In the formula: $\hat{k}$ represents a discrete time point and represents the current time step; t' represents the sampling time and the time interval between each time step; $\bar{I}''_{\alpha}(\hat{k})$、$\bar{V}'_{\alpha}(\hat{k})$、$\bar{V}''_{\alpha}(\hat{k})$ represents the alpha coordinate component, inverter output voltage, and inverter grid voltage at a specific discrete time point k ; $\bar{I}''_{\beta}(\hat{k})$、$\bar{V}'_{\beta}(\hat{k})$、$\bar{V}''_{\beta}(\hat{k})$ represents the beta coordinate component of grid connected current, inverter output voltage, and inverter grid voltage at a specific discrete time point k .

Using the forward Euler discretization of discrete time points, extrapolate the current reference value using vector angle compensation method:

$$\bar{I}'(\hat{k})=e^{j\hat{\theta}}\times\bar{I}''(\hat{k}) \quad (14)$$

In the formula: $\bar{I}'(\hat{k})$、$\bar{I}''(\hat{k})$ represents the current reference value and predicted current amplitude at a specific discrete time point, and represents the magnitude of the future current obtained according to the prediction algorithm; $\hat{\theta}$ represents the phase angle at a specific discrete time point and represents the phase information of the current.

Based on this, the minimum error value between current prediction and reference value is taken as the target of model predictive current control to achieve LVRT control on the AC side of photovoltaic grid connected power system. Table 1 shows the pseudocode for model predictive control.

Table 1. Pseudocode description.

Parameter/Component	Pseudocode Description
Prediction Horizon (N)	N = 10 # Predict outputs for the next 10 steps
Control Horizon (Nc)	Nc = 5 # Optimize control inputs for the first 5 steps, hold thereafter (Nc ≤ N)
Cost Function Form	J = Σ_{k=0}^{N-1} (...) # (Sum of tracking error and control effort terms)

Weight Matrices (Q, R)	Q = diag([1, 0.5]) # Output weights (*e.g.*, position, velocity)
	R = 0.1 * eye(m) # Control input weights

Terminal Weight (P)	P = 10 * Q # Terminal state penalty (optional)
Constraint Handling	u_min ≤ u(k) ≤ u_max # Control input limits Δu_min ≤ Δu(k) ≤ Δu_max # Control rate limits
Prediction Horizon (N)	N = 10 # Predict outputs for the next 10 steps

3. EXPERIMENTAL ANALYSIS

3.1 Experimental Environment Setup

A power system model of new energy photovoltaic grid connection was built based on Simulink simulation platform, and it was used as the experimental object for simulation analysis. Before simulation execution, the operating environment temperature of the photovoltaic array is defined as 26 ℃, and the input light intensity of the photovoltaic array unit is 1150W/m^2. Under standard conditions. Therefore, the maximum output power of multiple photovoltaic cells is 6452W, and the corresponding maximum power point current and voltage are 15.2A and 440V, respectively. In the simulation process, the MPPT algorithm for photovoltaic modules adopts the perturbation observation method, which is implemented by State Flow programming, and the model predictive control algorithm is implemented by s-function programming. The specific parameters of the new energy photovoltaic grid connected power system model constructed are shown in Table 2.

3.2 Low Voltage Ride through Control Effect Test

Causing a drop in grid voltage, which is within the normal range of 0-1.2s. The simulation waveform of active and reactive power output of the inverter before and after LVRT control during voltage drop are shown in Figure 4 using design methods.

From Figures 4a and 4b, it can be seen that the active power output by the inverter decreases during voltage drops. During the voltage drop period, the inverter also needs to send a certain amount of reactive power to the grid. Corresponding reactive power is emitted according to the depth of the grid voltage drop. The inverter realizes the coordinated control of active and reactive power; when the power grid voltage drops, the inverter performs reactive power priority control. Due to the requirement of linear output reactive current in photovoltaic grid connected power generation systems, the output reactive power will increase. Therefore, after using design methods to control, which to some extent supports the recovery of grid voltage.

Based on the same experimental environment, the simulated waveform of the photovoltaic array output before and after LVRT control during voltage drop are analyzed, as shown in Figure 5.

Table 2. Specific parameters of new energy photovoltaic grid connected power system model.

Power system model structure	Model parameters	Parameter values
Front stage booster circuit	PV side inductance/mH	3.2
	PV measurement capacitance/mF	2
	Switching frequency/kHZ	20
	Rated voltage of fast recovery diode/V	1000
	Rated current of fast recovery diode/A	1.2
	DC bus capacitance/mF	5.4
	DC bus voltage reference value/V	720
	Duty cycle range of Boost circuit	0.2-0.8
	MPPT control proportional and integral coefficients	0.1 and 0.05
Post inverter	Filter resistance/Ω	0.35
	Filter inductance/mH	5
	Grid-side voltage/V	420
	Bus voltage control outer ring ratio, integration factor	0.2 and 1
	Current control inner loop ratio, integral coefficient	0.5 and 0.05

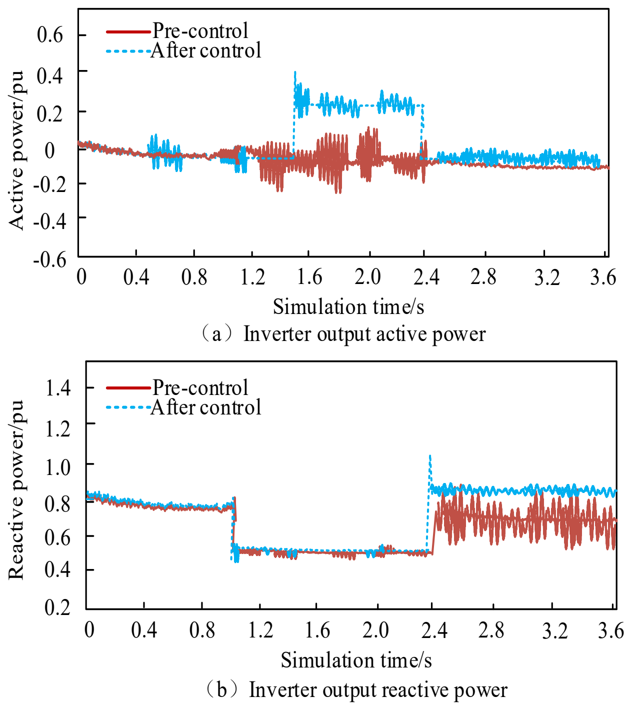

Fig. 4. Simulation waveforms of active and reactive power output of inverters before and after control.

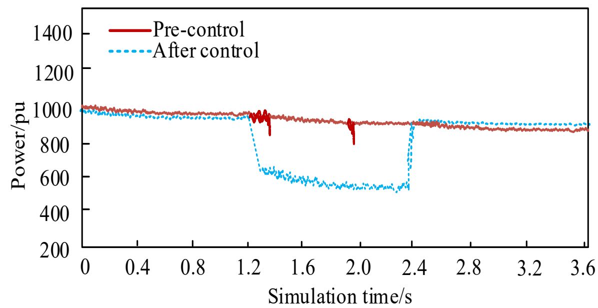

Fig. 5. Simulation waveform of photovoltaic array output before and after control.

As shown in Figure 5, if no design method is used for control, the output power of the photovoltaic array will always fluctuate around a small range of 1000pu (with a floating advance not exceeding 50pu). After adopting the design method for control, due to the use of power limiting control in the front stage, the photovoltaic array exits MPPT control during 1.2-2.4s, and the output power is reduced to around 625pu according to the degree of grid voltage drop.

Based on the above simulation environment, the methods of reference [4] and reference [5] are introduced as comparative methods to analyze the simulation waveform of the power grid before and after LVRT control during voltage drop period, as shown in Figure 6 and Figure 7.

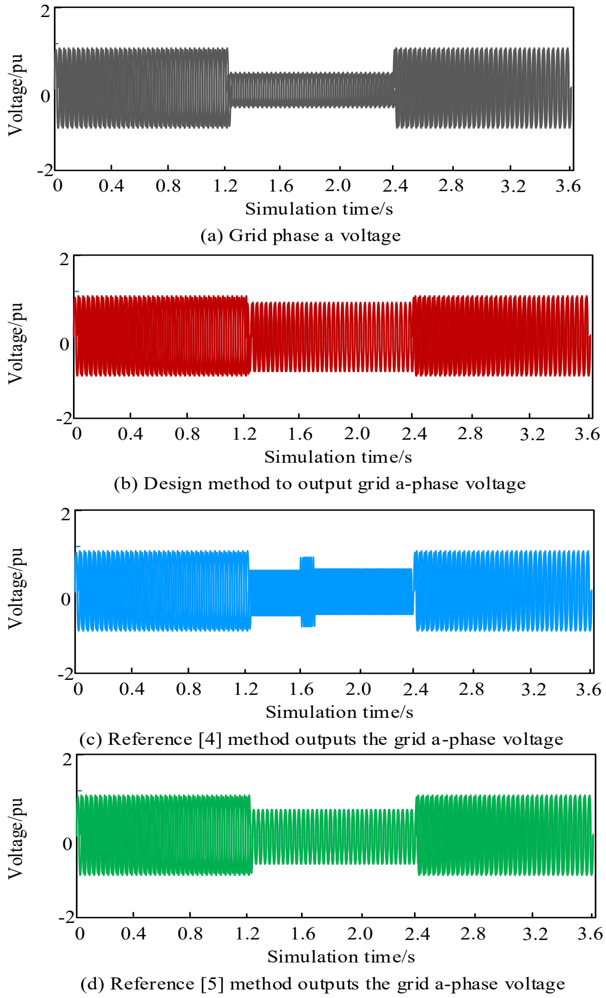

(a) Grid phase a voltage

(b) Design method to output grid a-phase voltage

(c) Reference [4] method outputs the grid a-phase voltage

(d) Reference [5] method outputs the grid a-phase voltage

Fig. 6. Waveform of phase A voltage output in the power grid before and after control.

From Figure 6, it can be seen that the grid voltage dropped to 0.45pu before adopting LVRT control, and dropped to 0.85pu after adopting design methods for control. Obviously, the voltage at the grid connection point has been restored to a certain extent. After using other methods for control, the degree of voltage drop in the power grid is similar to that of the original stone, and the recovery effect of grid voltage is poor.

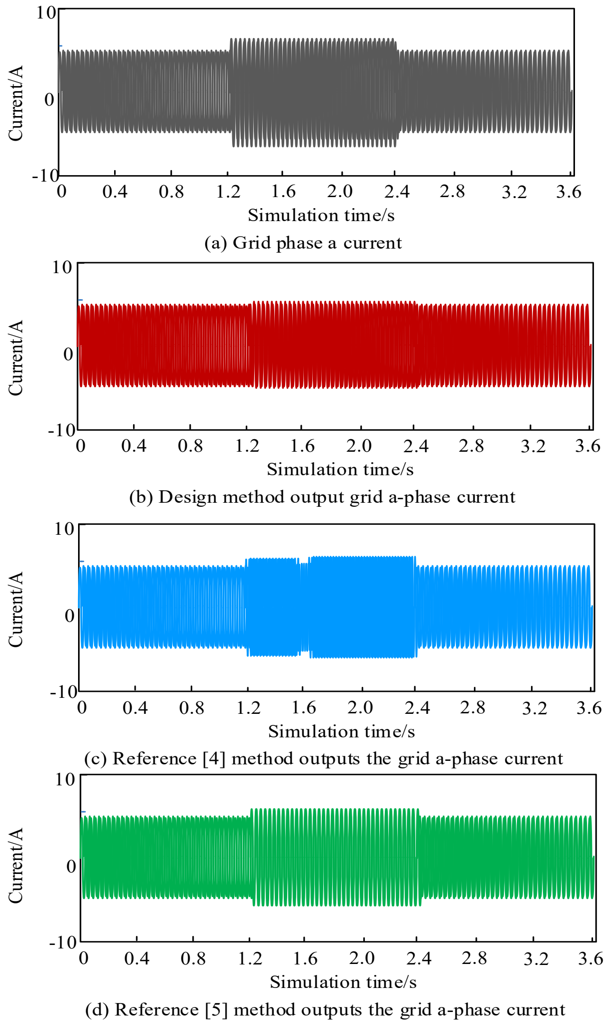

(a) Grid phase a current

(b) Design method output grid a-phase current

(c) Reference [4] method outputs the grid a-phase current

(d) Reference [5] method outputs the grid a-phase current

Fig. 7. Inverter output A-phase current waveform before and after control.

As shown in Figure 7, when the grid voltage drops, before adopting LVRT control, the output current of the inverter will suddenly increase, causing the current to exceed 1.1 times the rated current, resulting in the photovoltaic grid connected inverter operating off grid; After using design methods for control, the current rise is limited, and the output current of the inverter remains stable during the fault period, which can be well limited within the multiple control threshold of the rated current, thus protecting the power electronic components of the inverter and keeping it in grid connected operation. However, after using other methods for control, the current output by the inverter remains non-stationary during the fault period and cannot effectively control the rated current variation.

To comprehensively verify the effectiveness of the active low-voltage ride through (LVRT) strategy based on power direct control proposed in this paper in solving the problem of DC bus voltage instability caused by slow dynamic response of low-voltage ride through control strategy in new energy photovoltaic access power systems, a series of comparative experiments were designed. The experimental selection includes the reference [4] method, the reference [5] method, and the low-voltage ride through strategy based on Crowbar circuit labeled as traditional method 1. The low-voltage ride through strategy based on rotor side inverter control strategy is labeled as traditional method 2 as a reference. Under the same experimental environment and parameter settings, the dynamic response speed, DC bus voltage stability, and AC/DC power balance capability of different methods during grid side voltage drop are tested and compared. The experiment adopts the method of simulating power grid faults, setting up different levels of grid side voltage drop scenarios, and recording the key performance indicator data of each method in different scenarios. The results are shown in Table 3.

Table 3. Control performance analysis of different methods.

Experimental scenario (depth of voltage drop on the grid side)	Method	Dynamic response time (ms)	DC bus voltage fluctuation range (V)	AC/DC power balance time (ms)	Power tracking error (%)
Mild drop (20%)	Proposed Method	15	±5	20	1.2
	Reference [4] method	30	±12	40	3.5
	Reference [5] method	25	±10	35	2.8
	Traditional Method 1	40	±18	50	5.0
	Traditional Method 2	35	±15	45	4.2
Moderate drop (50%)	Proposed Method	20	±8	25	1.5
	Reference [4] method	45	±22	60	6.0
	Reference [5] method	35	±18	50	4.5
	Traditional Method 1	60	±30	75	8.0
	Traditional Method 2	50	±25	65	7.2
Severe drop (80%)	Proposed Method	25	±12	30	2.0
	Reference [4] method	60	±35	80	9.5
	Reference [5] method	45	±28	65	7.0
	Traditional Method 1	80	±45	100	12.0
	Traditional Method 2	70	±40	90	10.5

According to Table 3, the advantages of the active low-voltage ride through strategy based on direct power control proposed in this paper are fully demonstrated in mild, moderate, and severe grid side voltage drop scenarios. In terms of dynamic response time, the method proposed in this paper is significantly shorter than the methods in reference [4], reference [5], and various traditional LVRT strategies. For example, during mild drops, the method proposed in this paper only takes 15ms, while the method in reference [4] takes 30ms, and the traditional method 1 takes 40ms, which can more quickly perceive and respond to changes in grid voltage and avoid system instability; In terms of the fluctuation range of DC bus voltage, the method proposed in this paper is smaller than other comparative methods under different voltage drop depths. When there is a moderate drop, the method proposed in this paper is ± 8V, while the method in reference [4] reaches ± 22V, which can better maintain the stability of DC bus voltage, improve system reliability and power quality; In terms of power balance time on the AC/DC side, the method proposed in this paper performs well, achieving balance in only 30ms during severe drops, which is much lower than the 80ms of the method in reference [4] and the 100ms of the traditional method 1. By actively controlling the photovoltaic array and inverter to coordinate the output of the target power, power balance can be achieved faster and the impact of power imbalance can be reduced; In terms of power tracking error, the method proposed in this paper is at a relatively low level in various scenarios, with a slight drop of 1.2%, while the traditional method 1 achieves 5.0%. High precision tracking can improve energy utilization efficiency and reduce energy loss. In summary, through comparative experiments with various methods, it has been fully demonstrated that the strategy proposed in this paper has significant advantages in dynamic response speed, DC bus voltage stability, AC/DC power balance capability, and power tracking accuracy.

4. DISCUSSION

In the experimental analysis of this paper, based on Simulink simulation platform, the power system model of new energy photovoltaic grid connection is built, and the effectiveness of the proposed low voltage ride through (LVRT) control strategy is verified. The experimental results clearly show the coordinated control effect of the strategy on the active and reactive power output of the inverter during the grid voltage sag, as well as its flexible adjustment ability on the output power of the photovoltaic array.

Firstly, from the simulation waveform of the inverter output active and reactive power, the designed LVRT control strategy successfully realizes the coordinated control of active and reactive power. When the grid voltage drops, the inverter can respond quickly, reduce the active power output, and send the corresponding reactive power to the grid at the same time to support the recovery of grid voltage. This characteristic is of great significance to improve the stability and reliability of power system.

Secondly, the simulation waveform of photovoltaic array output power further verifies the effectiveness of the designed strategy. During the period of grid voltage sag, the photovoltaic array can exit the maximum power point tracking (MPPT) control by using the power limiting control strategy, and flexibly adjust the output power according to the degree of grid voltage sag. This flexible regulation capability helps to reduce the impact of grid faults on photovoltaic grid connected power generation system and improve the adaptability and robustness of the system.

In addition, compared with the methods proposed in references [4] and [5], the LVRT control strategy designed in this paper shows better performance in grid voltage recovery and inverter output current control. The experimental results show that after using this method, the voltage of the parallel node is more significantly restored, and the output current of the inverter remains stable during the fault period, which effectively avoids the problem of photovoltaic grid connected inverter off grid operation. This advantage is of great significance to improve the reliability and stability of photovoltaic grid connected power generation system.

5. CONCLUSION

To achieve effective low-voltage ride-through (LVRT) control for power systems with integrated renewable energy photovoltaics (PV) and ensure safe and stable grid operation, a PV grid-connected LVRT control strategy based on fast tracking of power reference values is proposed. By correspondingly controlling the front and rear stages of the power system with new energy PV integration, active and reactive power decoupling is achieved. Experimental results show that during voltage dips caused by grid faults, the unloading circuit suppresses DC side voltage fluctuations. After control using the designed method, the current output by the inverter can maintain a smooth transition, the PV power generation system can maintain grid-connected operation, and can compensate for a certain amount of reactive power, helping the grid quickly recover from faults and restore normal operating voltage.

However, there are also some work limitations in this study. Firstly, due to limitations in experimental conditions and time, the control strategy proposed in this paper has only been validated in simulation environments. However, there are significant differences between simulation environments and actual application scenarios, making it difficult to fully reproduce the complex operating conditions, transient uncertainties, and random characteristics of various sudden faults in the actual power grid in simulations. Therefore, this strategy has not yet been widely applied in practical power systems. In the future, it is necessary to conduct testing and verification in more practical scenarios to further confirm its effectiveness and reliability, especially focusing on the impact of transient uncertainties caused by load fluctuations, intermittent output of new energy in the actual power grid on the performance of control strategies. Secondly, with the continuous development of new energy technologies and the increasing complexity of power grid structures, the requirements for low-voltage ride through control strategies will also continue to increase.

In the future, in order to further promote the development of low voltage ride through control technology for new energy photovoltaic access to power system, the proposed control strategy can be applied to the actual power system for field test and verification, and necessary adjustment and optimization can be carried out according to the test results; At the same time, the characteristics of new energy power generation system and the operation law of power grid are deeply studied to develop more advanced and efficient low voltage ride through control strategy; In addition, we should strengthen cooperation and exchanges with other fields, jointly promote the innovation and development of new energy technologies, and contribute to the construction of a safe, stable and efficient smart grid.

REFERENCES

[1] Mahto K.K., Mahato B., Chandan B., Das B., Das P., Fotis G., Vita V., and Mann M., 2024. A new symmetrical source-based DC/AC converter with experimental verification. *Electronics* 13(10): 1975.

[2] Nandakumar N. and V.A. Tibbie Pon Symon. 2024. An implementation of inertia control strategy for grid-connected solar system using moth-flame optimization algorithm. *Automatika* 65(1): 206–216.

[3] Das D., Mahato B., Chandan B., Joshi H., Mahto K.K., Das P., Fotis G., Vita V., and Mann M., 2024. A new cascaded multilevel inverter for modular structure and reduced passive components. *Electronics* 13(17): 3566.

[4] Sun H., Lin X., Huang G., Zhang J., Liu D., Jiang K., and Kang Y., 2023. The transient instability mechanism and stability-enhanced LVRT control for VSC riding-through severe grid voltage sag. *IET Renewable Power Generation* 17(8): 2038–2049.

[5] Zheng X., Wu Z., Song G., Zhang J., Yang P., Zhang Z., and Lu X., 2024. Low-voltage ride-through control strategy for flywheel energy storage system. *Energy Science and Engineering* 12(4): 1486–1502.

[6] Ni Z., Abuelnaga A.H., Badawi S., Yuan S., Narimani M., Sayed-Ahmed A., Cheng Z., and Zargari N.R., 2023. A new low switching frequency control of regenerative CHB drive with low-voltage ride-through capability. *IEEE Transactions on Power Electronics* 38(2): 1973–1983.

[7] Pal A., Pal D., and Panigrahi B.K., 2023. A current saturation strategy for enhancing the low voltage ride-through capability of grid-forming inverters.

IEEE Transactions on Circuits and Systems II: *Express Briefs* 70(3): 1009–1013.

[8] Chakraborty S., Mukhopadhyay S., and Biswas S.K., 2023. A hybrid compensator for unbalanced AC distribution system with renewable power. *IEEE Transactions on Industry Applications* 59(1, Pt.1): 544–553.

[9] Krishna C.R.V., Mikkili S., and Bonthagorla P.K., 2023. Modeling, controlling approaches, modulation schemes, and applications of modular multilevel converter: Review. *Journal of Control, Automation and Electrical Systems* 34(1): 189–215.

[10] Tajjour S., Chandel S.S., and Thakur C.N., 2023. Power generation enhancement analysis of a 400 kWp grid-connected rooftop photovoltaic power plant in a hilly terrain of India. *Energy for Sustainable Development* 77: 101333–101333.17.

[11] Boruah D. and S.S. Chandel. 2024 Techno-economic feasibility analysis of a commercial grid-connected photovoltaic plant with battery energy storage-achieving a net zero energy system. *Journal of Energy Storage* 77: 109984.

[12] Mahinda M.W., Wanjiru E.M., and Njiri J.G., 2023. Optimal control of a grid-connected photovoltaic agricultural water pumping system. *Journal of Engineering and Applied Science* 70(1).

[13] Zhang X., Huang C., and Shen J., 2023. Energy optimal management of microgrid with high photovoltaic penetration. *IEEE Transactions on Industry Applications* 59(1, Pt.1): 128–137.

[14] Wang Y., Wang X., Li S., Ma X., Chen Y., and Liu S., 2024. Optimization model for harmonic mitigation based on PV-ESS collaboration in small distribution systems. *Applied Energy* 356: 122409.

[15] Mazlan M.A.A. and N.Y. Dahlan. 2023. Energy management strategies of solar rooftop campus with battery energy storage system (BESS) and EV supply equipment (EVSE) using HOMER. *IOP Conference Series*: *Earth and Environmental Science* 1281(1).

[16] Chen J. and H.Q. Wei. 2023. Simulation of low voltage ride through test algorithm for electrical equipment of power plant. *Computer Simulation* 40(7): 67–70, 81.

[17] Phan N.M.L., Tung D.N., Thanh T.N., and Vu T.T., 2023. ANFIS wind speed estimator-based output feedback near-optimal MPPT control for PMSG wind turbine. *Journal of Control*, *Automation and Electrical Systems* 34(3): 588–598.

[18] Mbarki B., Fethi F., and Chrouta J.Z.A., 2024. Adaptive neuro-fuzzy inference system algorithm-based robust terminal sliding mode control MPPT for a photovoltaic system. *Transactions of the Institute of Measurement and Control* 46(2): 316–325.

[19] Priya D. and A. Sumathi. 2024. Reverse flow transition control mechanism with maximum power point controlling (MPPT) technique for solar PV application. *Journal of the Chinese Institute of Engineers* 47(1): 37–50.

[20] Çelik K., Demirtas M., and Öztürk N., 2023. Analytical MPPT control and comparative analysis for PV panel connected to DC microgrid. *Electric Power Components and Systems* 51(11–15): 1075–1088.

[21] Deboucha H., Kermadi M., Mekhilef S., and Belaid S.L., 2023. Ultra-fast and accurate MPPT control structure for mobile PV system under fast-changing atmospheric conditions. *IEEE Transactions on Sustainable Energy* 14(4): 2168–2176.

[22] Mamouri L., Mesbahi T., and Frick V.,2 024. MPPT technique with improved FOCV control applied to a full active rectifier for low-voltage piezoelectric energy harvesting. *IEEE Transactions on Circuits and Systems II*: *Express Briefs* 71(2): 532–536.

[23] Hata N., Belhaouchet N., and Sayah S., 2023. Design and experimental validation of an efficient control based on variable step size P&O MPPT technique and predictive current controller for a single-phase grid-connected photovoltaic system. *Electrical Engineering* 105(5): 2637–2652.

[24] Imtiaz S., Yang L., Azib Khan H.M., Mudassir Munir H., Alharbi M., and Jamil M. 2024. Wind-assisted microgrid grid code compliance employing a hybrid Particle swarm optimization-Artificial hummingbird algorithm optimizer-tuned STATCOM. *Wind Energy* 27(7): 711–732.

[25] Kumaresan A., Tafti H., Beniwal N., Gorla N., Farivar G., Pou J., and Konstantinou G. 2023. Improved secant-based global flexible power point tracking in photovoltaic systems under partial shading conditions. *IEEE Transactions on Power Electronics* 38(8, Pt.2): 10383–10395.

[26] Chatri C., Labbadi M., and Ouassaid M., 2023. Improved high-order integral fast terminal sliding mode-based disturbance-observer for the tracking problem of PMSG in WECS. *International Journal of Electrical Power & Energy Systems* 144: 108514.